12872–12884 *Nucleic Acids Research, 2022, Vol. 50, No. 22* *Published online 13 December 2022*
https://doi.org/10.1093/nar/gkac1169

The *Escherichia coli* clamp loader rapidly remodels SSB on DNA to load clamps

Elijah S.P. Newcomb, Lauren G. Douma, Leslie A. Morris and Linda B. Bloom*

Department of Biochemistry and Molecular Biology, University of Florida, Gainesville, FL 32610-0245, USA

Received October 13, 2022; Editorial Decision November 10, 2022; Accepted December 06, 2022

ABSTRACT

Single-stranded DNA binding proteins (SSBs) avidly bind ssDNA and yet enzymes that need to act during DNA replication and repair are not generally impeded by SSB, and are often stimulated by SSB. Here, the effects of *Escherichia coli* SSB on the activities of the DNA polymerase processivity clamp loader were investigated. SSB enhances binding of the clamp loader to DNA by increasing the lifetime on DNA. Clamp loading was measured on DNA substrates that differed in length of ssDNA overhangs to permit SSB binding in different binding modes. Even though SSB binds DNA adjacent to single-stranded/double-stranded DNA junctions where clamps are loaded, the rate of clamp loading on DNA was not affected by SSB on any of the DNA substrates. Direct measurements of the relative timing of DNA-SSB remodeling and enzyme–DNA binding showed that the clamp loader rapidly remodels SSB on DNA such that SSB has little effect on DNA binding rates. However, when SSB was mutated to reduce protein–protein interactions with the clamp loader, clamp loading was inhibited by impeding binding of the clamp loader to DNA. Thus, protein–protein interactions between the clamp loader and SSB facilitate rapid DNA-SSB remodeling to allow rapid clamp loader-DNA binding and clamp loading.

INTRODUCTION

Single-stranded DNA binding proteins (SSBs) are found in all domains of life and in many DNA viruses. SSBs rapidly and avidly bind single-stranded DNA (ssDNA) that forms as an intermediate of normal cellular processes such as DNA replication and repair (reviewed in (1–3)). In doing so, SSBs serve structural functions including preventing ssDNA from forming secondary structures that may be detrimental to DNA metabolism and protecting ssDNA from nucleases. Enzymes required for DNA metabolism need to be able to act on SSB-coated DNA, and another important function of SSBs is to coordinate the activities of enzymes and proteins required for these processes. Rather than blocking enzymes that act on DNA, SSBs often stimulate their activities via direct protein–protein interactions (reviewed in (4,5)), but there is still much that is not known about mechanisms by which SSBs influence enzyme activity. Mechanisms by which the *Escherichia coli* DNA polymerase processivity clamp loader, γ complex ($\gamma_3\delta\delta'\chi\psi$ subunits), interacts with SSB to load clamps on DNA is investigated here.

SSBs bind ssDNA with high affinity through a common oligonucleotide/oligosaccharide protein fold (OB-fold). *E. coli* SSB is composed of four identical subunits, each of which possesses an OB-fold in the N-terminal domain that can bind ssDNA. SSB binds DNA three main modes, $(SSB)_{35}$, $(SSB)_{56}$ and $(SSB)_{65}$, that differ in the number of times DNA is wrapped around the tetramer and the number of nucleotides that are occluded by the protein, 35-, 56- and 65-nt, respectively (6–8). Two of the four OB-folds are bound in the cooperative $(SSB)_{35}$ binding mode, and all four OB-folds engage DNA in the $(SSB)_{65}$ binding mode where DNA is bound with lower cooperativity. *In vitro* at physiological salt concentrations, SSB binds ssDNA stoichiometrically with a binding constant too high to measure accurately (9). Although SSB binds ssDNA with high affinity, SSB-DNA interactions are dynamic in that SSB can slide along DNA and spontaneously switch binding modes (10,11). Enzymes may take advantage of these DNA-SSB dynamics to gain access to DNA which may help prevent SSB from competing with enzymes for DNA binding.

The C-terminal end of *E. coli* SSB contains two structural features, an intrinsically disordered linker region and a conserved sequence motif at the very end of the protein or C-tail. The conservation of the C-tail sequence likely reflects its function of mediating protein–protein interactions. This 8–10 amino acid region of the protein binds directly to a number of enzymes that are involved in *E. coli* DNA metabolism including DNA polymerases and primase (12–14), nucleases (15,16), DNA helicases (17,18), recombination proteins (19–22), replication restart proteins (23–26), and uracil DNA glycosylase (27). The χ subunit of the *E. coli* DNA polymerase processivity clamp

*To whom correspondence should be addressed. Tel: +1 352 294 8379; Fax: +1 352 392 2953; Email: lbloom@ufl.edu
Present address: Leslie A. Morris, School of Medicine, University of Louisville, Louisville, KY 40202, USA.

loader is another example of an SSB-interacting protein (SIP) that binds the C-tail (28,29). Specifically, the C-terminal Phe residue (Phe-177) binds a hydrophobic pocket on χ, and acidic groups in the C-tail interact with positively charged residues of χ (30,31). The general features of this binding mechanism have been observed for other SIPs that have been co-crystalized with SSB C-tail peptides (15,16,18,23,32). The essential nature of SSB-protein interactions is highlighted by the observation that deletion of the last 10 amino acids of SSB is lethal to *E. coli* even though this SSB C-tail deletion mutant retains high affinity DNA binding activity (33). While interactions between the C-tail and SIPs seem to be the predominant mechanism for binding, a second type of binding interaction has recently been identified for some enzymes. These SIPs may interact with the intrinsically disordered linker region of SSB (34–37). Regardless of the binding mechanism, physical interactions between SSB and SIPs may help target SIPs to DNA sites where they are needed and stimulate enzyme activity.

The clamp loader is a component of the DNA polymerase III holoenzyme along with the DNA polymerases that catalyze synthesis of DNA during replication. The function of the clamp loader is to load the β-sliding clamp onto DNA, and the β-sliding clamp in turn binds DNA polymerases to increase the processivity of DNA synthesis. The mechanical clamp loading reaction is powered by ATP binding and hydrolysis, and the clamp loader is a member of the AAA+ family of ATPases. Physical and functional interactions between the DNA polymerase III holoenzyme and SSB are mediated by the χ subunit of the clamp loader as discussed above (28,29,38). These χ-SSB interactions affect the activity of the DNA polymerase III holoenzyme in a number of ways including (i) increasing the salt resistance of DNA synthesis, (ii) mediating the switch from primase to polymerase, (iii) helping to chaperone the polymerase to a newly loaded clamp and (iv) coupling leading and lagging strand synthesis (28,30,38–40). Given that χ is a subunit of the clamp loader portion of the holoenzyme, this work focuses effects of SSB on the enzymatic activity of the clamp loader and clamp loader-DNA interactions.

The clamp loader contains seven polypeptides, three copies of the DnaX subunit and one copy each of the δ, δ', ψ and χ subunits (41,42). Two different forms of DnaX are made in the cell, a full-length form (τ) and a truncated form (γ) made by a translational frameshift (43–45). The γ protein is about 2/3 length of τ and contains the AAA+ ATPase domains needed for clamp loading. The additional C-terminal domains of τ mediate interactions with the helicase and the polymerase (46–53). In the context of the holoenzyme, the clamp loader likely contains two copies of τ and one copy of γ (54). By binding the α subunit of DNA polymerase III, the τ subunits tether two polymerases to the clamp loader. Active clamp loaders can be made using any combination of DnaX subunits (55). The γ complex clamp loader ($\gamma_3\delta\delta'\chi\psi$ subunits) is used in this study because it is fully active as a clamp loader and lacks the C-terminal regions of τ that are subject to proteolysis during clamp loader purification giving heterogeneous clamp loader protein preparations. In this work, mechanisms by which the γ complex clamp loader interacts with and loads clamps on DNA bound by SSB are investigated.

MATERIALS AND METHODS

Buffers

Reaction buffers contained 20 mM Tris-HCl pH 7.5, 50 mM NaCl, 8 mM $MgCl_2$, 0.5 mM ATP or ATPγS, 5 mM DTT, 40 μg/ml BSA and 4% glycerol. Clamp closing reactions also contained 0.5 mM EDTA.

Proteins and oligonucleotides

The γ complex clamp loader ($\gamma_3\delta\delta'\chi\psi$ subunits) and β-clamp were expressed and purified as described (56–58). A unique Cys residue was incorporated into SSB by site-directed mutagenesis of Ala-122 to Cys. The SSBΔC1 expression vector was a gift of the Keck laboratory. Wild-type and mutant SSB proteins were expressed and purified as described (59). Unlabeled protein concentrations were determined by measuring the absorbance at 280 nm under denaturing conditions and using extinction coefficients of 220 050 M^{-1} cm^{-1} for γ complex (60), 14 700 $M^{-1}cm^{-1}$ for β (58) and 28 300 M^{-1} cm^{-1} for wt SSB (8). Empirical titrations of ssDNA with WT SSB in clamp closing and FRET assays showed that 1.5 molar equivalents of SSB ensured all ssDNA was bound. Whenever SSB was present in reactions, SSB was bound to DNA by pre-incubating the two prior to adding the other reagents. Oligonucleotides were purchased from Integrated DNA Technologies and purified by PAGE or HPLC. Fluorescein-dT was incorporated into oligonucleotides during synthesis. AF488 was covalently attached to an oligonucleotide containing an C6 amino linker on the 5′ position of dT and purified as described previously (61).

Labeling proteins with fluorophores

Unique surface Cys residues were introduced into β for clamp closing (β-R103C/I305C/C260S/C333S) (62), β for clamp loader-clamp binding DNA: β-I305C/C260S/C333S (62), and SSB for DNA-SSB remodeling (SSB-A122C) (63). In some experiments, WT β was labeled on Cys-333 for FRET DNA binding assays. Proteins were labeled on Cys residues with maleimide derivatives of Alexa Fluor 488 (β-$AF488_2$) or Alexa Fluor 647 (β-AF647 and SSB-AF647). Labeled proteins were purified as described previously for β using a desalting column (BioGel P6-DG, BioRad), anion exchange chromatography (HiTrap Q, Cytiva), and dialysis to remove excess fluorophore from proteins after labeling (62). Labeled protein concentrations were determined by using a Bradford-type assay (Bio-Rad Protein Assay) with unlabeled proteins (β or SSB) as standards or from the absorbance of β at 280 nm for β-AF647.

Equilibrium clamp loader DNA binding assays

DNA was labeled with a fluorescein donor at a dT 20-nt from the 3′ recessed end and annealed to a complementary strand to form a 30-nucleotide duplex with a 65-nt ss poly-dT 5′ overhang. The β-clamp was labeled at Cys-333 with an AF647 acceptor. Steady-state fluorescence was measured using a Photon Technology International QuantaMaster 1 fluorimeter with a 3 nm bandpass and measuring emission from 505 to 750 nm when exciting at 495 nm. Spectra for

DNA or DNA-SSB in assay buffer containing ATPγS was measured to provide a signal for free DNA before adding β-AF647 and γ complex to measure equilibrium binding. Sufficient β-AF647 was added to ensure that at least 95% of the γ complex was bound by β assuming a K_d of 3 nM for γ complex-β dissociation (64). Titration data was analyzed and graphed using KaleidaGraph. Relative fluorescence intensity values at 520 nm were calculated by dividing the signal for β, γ complex and DNA (or DNA-SSB) by the signal for free DNA (or DNA-SSB). These values were plotted as a function of clamp loader concentration and fit to a quadratic curve (Equation (1)) assuming a 1:1 protein:DNA binding stoichiometry to calculate the K_d value where D_0 is the total DNA concentration, γ_0 is the total γ complex concentration and S_b and S_f are the fluorescence signals for bound and free DNA, respectively.

$$y = \frac{D_o + \gamma_o + K_d - \sqrt{(D_o + \gamma_o + K_d)^2 - 4D_o\gamma_o}}{2D_o}(S_b - S_f) + S_f \quad (1)$$

Clamp closing reactions

A sequential mixing scheme was used where the clamp loader, β-AF488$_2$ and ATP were mixed and preincubated for 4 s prior to adding DNA and excess unlabeled clamp to measure rates of clamp closing. In DNA titration trials, final concentrations were 20nM clamp loader, 20 nM β-AF488$_2$, 200 nM unlabeled β, 40 nM, 80 nM or 160 nM DNA, and 1.5 molar equivalents of SSB or SSBΔC1 per DNA molecule when present. Additionally, overhang lengths of 35, 65 and 80 nt were tested at 40 nM DNA. Experiments with the 80-nt ssDNA overhang were done with both 1.5 and 5 molecules of SSB per DNA molecule. The decrease in AF488 fluorescence that occurs when clamps are closed on DNA was measured as a function of time using an Applied Photophysics SX20MV stopped-flow by exciting AF488 at 495 nm using a 3.7 nm bandpass. Fluorescence emission measured using a 515-nm long pass filter. Data was collected every millisecond over four seconds, for a total of 4000 time points. Time courses were fit to double exponential decays (Equation (2)) for wild-type SSB to estimate the rates of decrease in fluorescence where a_{fast} and a_{slow} are the amplitudes associated with the fast and slow phases and k_{fast} and k_{slow} are the rates of the fast and slow phases, respectively, and c is a constant. Double exponential decays did not improve the quality of empirical fits of time courses reactions with SSBΔC1 so the simpler single exponential fits were used.

$$y = a_{fast}\left(1 - e^{tk_{fast}}\right) + a_{slow}\left(1 - e^{tk_{slow}}\right) + c \quad (2)$$

Stopped-flow FRET experimental set-up

An Applied Photophysics SX20MV stopped-flow was used in single-mix mode to mix equal volumes (60 μl) from two different syringes. The pressure was held throughout the data collection period. Fluorescein was excited at 495 nm with a bandpass of 5.5 nm. Emission was measured using a 540 nm filter with a bandpass of 50 nm manufactured by Edmund Optics.

DNA binding reactions

Single mix reactions were done in which a solution γ complex and β-AF647 was added to a solution of DNA or DNA-SSB. Final concentrations were 20 nM DNA, 30 nM SSB when present, 0.5 mM ATPγS, 20, 40 or 80 nM γ complex along with 100 nM β-AF647 in reactions with 20 and 40 nM γ complex or 200 nM β-AF647 in reactions with 80 nM γ complex. Data was collected using a split timebase over 11 s in which the first 1000 points were collected at a 1 ms interval followed by 1000 points collected at a 10 ms interval.

DNA dissociation reactions

Single mix reactions were done in which a solution of DNA-F with or without SSB, γ complex, β-AF647 and ATPγS was mixed with a solution of unlabeled DNA or DNA-SSB and ATPγS. Final concentrations were 20 nM DNA-F with or without 30 nM SSB, 40 nM γ complex, and 100 nM β-AF647 400 nM unlabeled DNA (same sequence as labeled DNA) or DNA-SSB, and 0.5 mM ATPYS. For DNA-SSB reactions, data was collected using a split time base in which 1000 points were collected at a 1 ms interval followed by 10 000 points collected at a 6 ms interval (60 s total). For DNA only reactions, 10 000 points were collected at a 2 ms interval (20 s total).

Equilibrium DNA-SSB remodeling

The DNA substrate consisted of 30-nt duplex labeled with AF488 on dT 7-nt from the 3′ recessed end and a 35-nt 5′ ss dT overhang. Fluorescence emission spectra were measured from 505 to 735 nm when exciting at 495 nm and using a bandpass of 3 or 4 nm. DNA substrates were titrated with SSB-AF647 until the fluorescence reached a minimum value. The magnitude of the quench that occurs when SSB-AF647 binds DNA-AF488 was calculated from the difference in intensity at 520 nm for free DNA and DNA that was saturated with SSB-AF647. Final concentrations were 10 nM DNA-AF488 and 0–200 nM SSB-AF647.

DNA-SSB remodeling was measured by adding a solution of γ complex and β to a solution of DNA-AF488, SSB-AF647 and ATPγS. Spectra for DNA-SSB were measured before and after addition of γ complex and β. The relative fluorescence value for the remodeled complex was calculated from the ratio of the intensity at 520 nM for DNA-SSB plus γ complex and β divided by that for DNA-SSB only. Final concentrations were 10 nM DNA-AF488, 50 nM SSB-AF647, 0–100 nM γ complex, 200 nM β and 0.5 mM ATPγS.

Real-time DNA-SSB remodeling reactions

The DNA substrate consisted of a 30-nt duplex labeled with fluorescein on dT 7-nt from the 3′ recessed end and a 35-nt 5′ ss dT overhang. Single mix reactions were done in which a solution containing γ complex, β, and ATPγS was mixed with a solution of DNA-F bound by SSB-AF647 and ATPγS. Final concentrations were 40 nM γ complex, 100 nM β, 20 nM fluorescein labeled DNA, 30 nM SSB labeled with AF647, and 0.5 mM ATPγS. Four thousand data points were collected at a 1 ms interval (4 s total).

Reproducibility and error

Experiments were generally done three times. As an additional measure of robustness, measurements were made by varying the order of addition (equilibrium) or comparing different reactions side-by-side (kinetic) to rule out systematic effects due to methods. In equilibrium titration experiments, the order in which various concentrations of titrant were added to reactions differed between replicate experiments. In kinetic experiments, different reactions were measured in side-by-side experiments in different replicates. For example, in one replicate, the same DNA concentration was used in reactions with and without SSB and in another replicate, different DNA concentrations were compared side-by-side. Representative kinetic traces are shown. Rate and equilibrium constants were calculated from three independent experiments and are reported as the average with standard deviation. Titration data for each of the three replicate experiments are plotted along with the average and standard deviation.

RESULTS

Clamp loader–clamp binding to DNA is enhanced by wild-type SSB and inhibited by a SSB C-tail mutant, SSBΔC1

The *E. coli* clamp loader loads clamps on ss/ds DNA junctions with 5′ ss DNA overhangs to which SSB would typically be bound *in vivo*. Clamp loader binding to DNA and to DNA bound by SSB (DNA-SSB) was measured under equilibrium conditions. The *E. coli* γ complex clamp loader, composed of $\gamma_3\delta\delta'\chi\psi$ subunits, was used for all the experiments in this study. Although SSB binds DNA stoichiometrically at the concentrations used in this work, an excess of SSB was used (1.5 molecules of SSB per molecule of DNA) to ensure that all DNA was bound by SSB. A DNA substrate with a 30-base pair (bp) duplex region and a 65-nucleotide (nt) single-stranded dT (ss dT_{65}) 5′ overhang was used to allow SSB to bind in the $(SSB)_{35}$, $(SSB)_{56}$ or $(SSB)_{65}$ binding modes (6–8). Equilibrium binding of the clamp loader to DNA was measured using a fluorescence resonance energy transfer (FRET) assay to determine how SSB affects access of the clamp loader to ss/ds DNA junctions. Briefly, DNA was labeled with a fluorescein donor (DNA-F) 20 nucleotides from the 3′-recessed end and the β-clamp was labeled with an Alexa Fluor 647 acceptor (β-AF647). Binding of the clamp loader-β-AF647 complex to DNA quenches donor fluorescence. ATP was replaced by the nonhydrolyzable ATP analog, ATPγS, to inhibit ATP hydrolysis by the clamp loader and permit measurement of the clamp loader-clamp complex binding to DNA without loading clamps. When DNA-F (Figure 1, upper panel) or DNA-F bound by SSB (DNA-SSB) (Figure 1, middle panel) was titrated with γ complex and β-AF647, donor fluorescence decreased with increasing clamp loader concentration due to FRET. Binding isotherms were fit to Equation (1) (Materials and Methods) describing 1:1 protein:DNA binding to calculate dissociation constants (K_d) of 30.6 ± 19.7 nM for DNA and 6.6 ± 1.7 nM for DNA-SSB showing that SSB enhances binding of the clamp loader to DNA. The decrease in fluorescence intensity in the binding isotherm for DNA-SSB is steeper than the slope described by this simple 1:1 binding model suggesting that

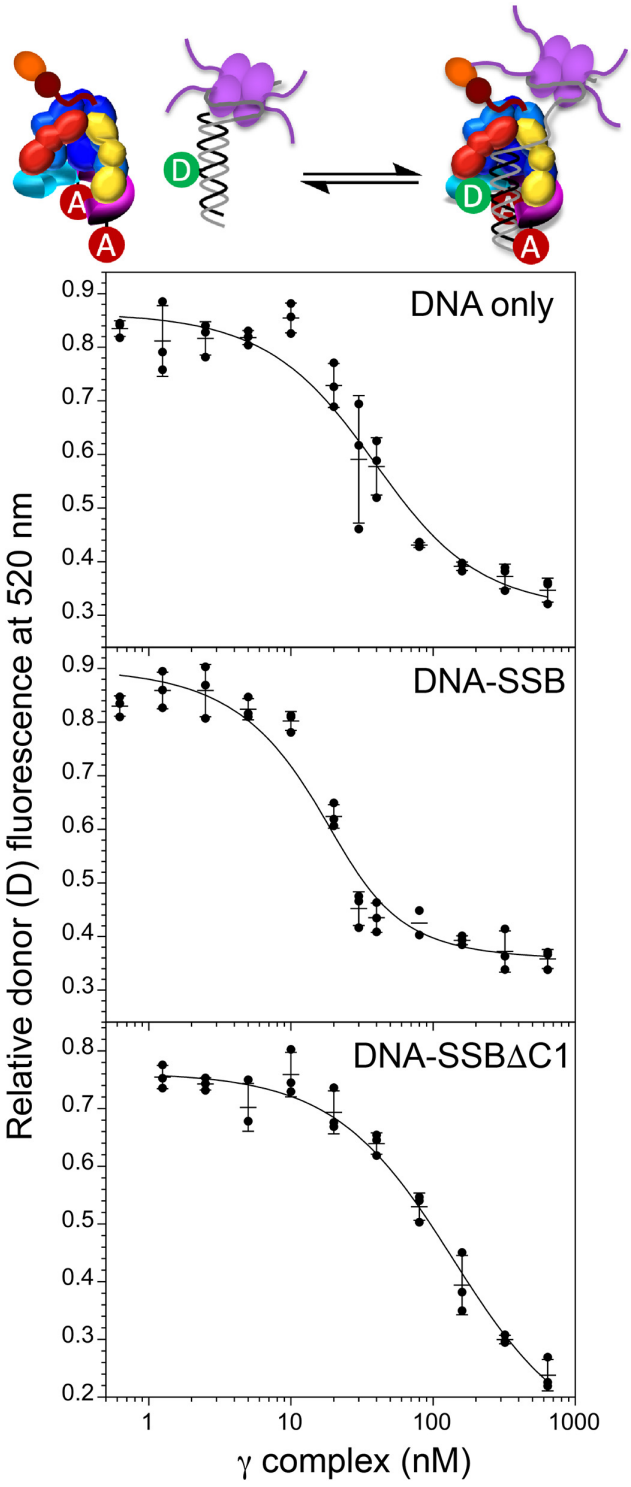

Figure 1. Equilibrium binding of a clamp loader-clamp complex to DNA or DNA-SSB measured by FRET. Fluorescein-labeled DNA (DNA-F) was titrated with the γ complex and AF647-labeled clamp to measure DNA binding in reactions containing 20 nM DNA (*upper panel*), 20 nM DNA and 30 nM wt SSB (*middle panel*), 20 nM DNA and 30 nM SSBΔC1 (*lower panel*) in the presence of 0.5 mM ATPγS. The concentration of γ complex was varied, and the concentration of β-AF647 was sufficient to ensure that at least 95% of the γ complex was bound by β. Data points show values for three independent titrations for each condition. Average donor intensity values (horizontal line) and standard deviations (error bars) are plotted also.

SSB may have a cooperative effect on clamp loader-DNA binding. The χ subunit of the clamp loader binds the acidic C-terminal end of SSB and the last residue, Phe-177, binds a hydrophobic pocket on χ (28,30,38). Binding of the clamp loader-clamp to a DNA substrate bound by a SSB mutant that lacks Phe-177 (SSBΔC1) reduced binding of the clamp loader-clamp to DNA (Figure 1, lower panel). Fitting the binding data for DNA-SSBΔC1 to a 1:1 protein:DNA binding model yields a K_d of 140 ± 60 nM. The SSB mutation also affects the shape of the binding isotherm such that the slope of the decrease in fluorescence is not as steep as for wt SSB and fit to the 1:1 protein:DNA binding model.

SSB does not increase the binding rate of the clamp loader to DNA, but instead increases the lifetime of the clamp loader-clamp complex on DNA

The enhancement of clamp loader–DNA binding by SSB could be due to increasing the on-rate, decreasing the off-rate, or a combination of the two. To determine how SSB affects DNA binding rates, the FRET-based DNA binding assay was used to measure binding as a function of time at three different DNA or DNA-SSB concentrations (Figure 2). The same DNA substrate with a 30-bp duplex and a ss dT_{65} 5′ overhang was used. Overall, SSB had a relatively small effect on binding reactions. At the lowest clamp loader concentration (20 nM), the difference in observed binding rates was the greatest with binding being *slower* for the DNA-SSB substrate. With increasing concentrations of clamp loader, rates of binding increase as expected for a bimolecular reaction. These data show that SSB does not increase DNA binding rates to enhance clamp loader-DNA binding.

Given that SSB did not increase DNA binding rates, the expectation is that the enhanced binding affinity for DNA-SSB is due to slower dissociation of the clamp loader-clamp from DNA-SSB than DNA. To test this possibility, clamp loader–clamp dissociation from DNA and DNA-SSB was measured using the FRET-based DNA binding assay. An excess of unlabeled DNA trap and ATPγS was added to a solution containing γ complex, β-AF647, DNA-F and ATPγS. In experiments containing SSB, the DNA trap was pre-bound with SSB to avoid the possibility of transfer of SSB from the substrate to the trap. As predicted, the clamp loader-clamp complex dissociates from DNA faster than from DNA-SSB (Figure 3). Fitting the time courses for dissociation to exponentials gave an average rate of 0.46 ± 0.05 s^{-1} for naked DNA and 0.14 ± 0.02 s^{-1} for DNA-SSB, about 3 times slower when SSB is bound to DNA.

Clamp loading is not affected by SSB bound to DNA

In the absence of ATP hydrolysis, SSB enhances binding of the clamp loader-clamp to DNA by increasing the lifetime of the proteins on DNA. To determine how SSB affects clamp loading in reactions with ATP, clamp closing around DNA and DNA-SSB was measured. Briefly, the β-clamp was labeled on both sides of the dimer interfaces with Alexa Fluor 488 (AF488) such that when the β-$AF488_2$ clamp is bound to the clamp loader and open, a pair of

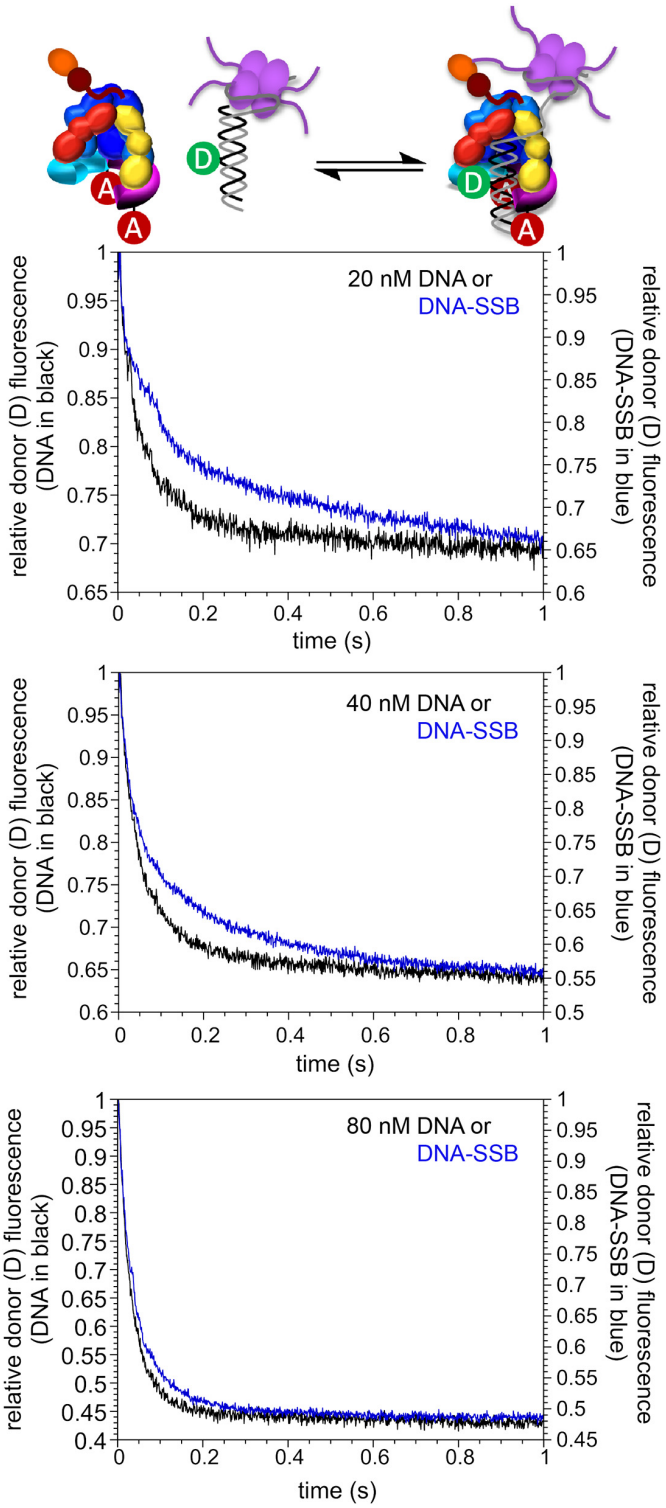

Figure 2. Real time binding of clamp loader–clamp complexes to DNA and DNA-SSB. Representative time courses show the decrease in donor fluorescence that occurs when DNA-F is bound by a clamp loader-clamp complex containing β-AF647 in reactions with (blue) and without (black) SSB. Binding reactions contained 20 nM γ complex and 100 nM β-AF647 (top panel), 40 nM γ complex and 100 nM β-AF647 (middle panel), and 80 nM γ complex and 200 nM β-AF647 (bottom panel), 20 nM DNA-F, 30 nM SSB when present, and 0.5 mM ATPγS.

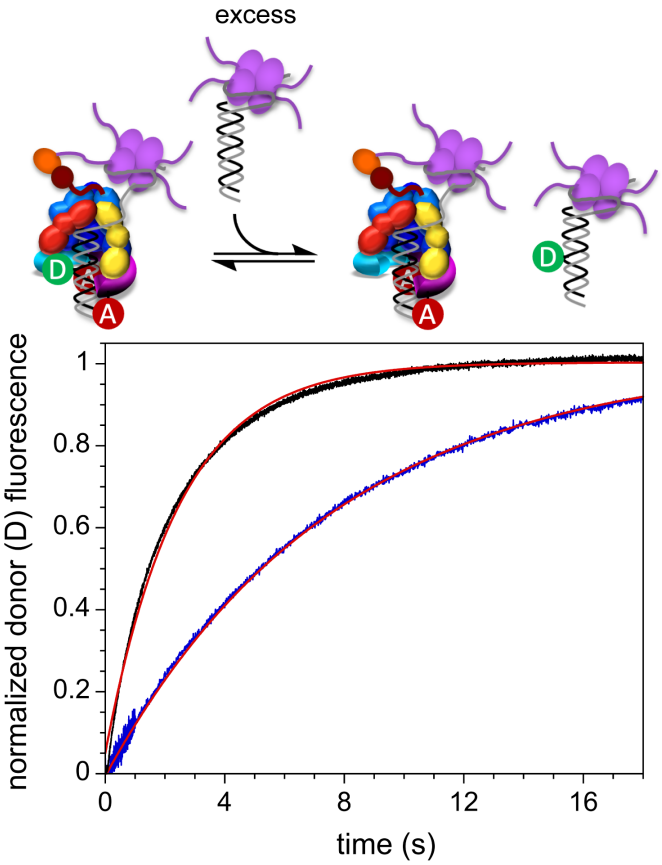

Figure 3. Clamp loader-clamp complexes dissociation from DNA (black) and DNA-SSB (blue). Representative time courses are shown from reactions in which an excess of unlabeled DNA or DNA-SSB trap was added to a solution of DNA-F or DNA-F-SSB, respectively, bound by γ complex and β-AF647. Final concentrations were 40 nM γ complex clamp loader, 100 nM β-AF647 clamp, 20 nM DNA-F, 30 nM SSB when present, 400 nM unlabeled DNA or 400 nM DNA-SSB trap and 0.5 mM ATPγS. Solid red lines through data show single exponential fits used to calculate dissociation rates.

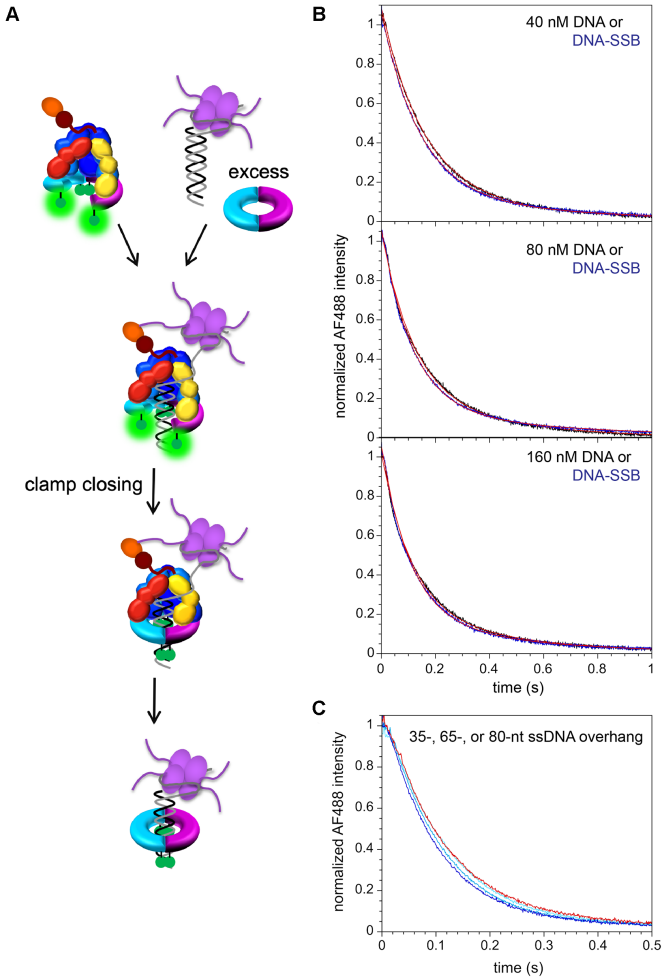

Figure 4. Clamp loading on DNA without and with bound SSB. (**A**) The reaction scheme for clamp closing is shown. The clamp loader was pre-incubated with β-AF488$_2$ and ATP for 4 s to form an open clamp loader-clamp complex prior to adding DNA or DNA-SSB along with an excess of unlabeled β-clamp to limit reactions to a single turnover. (**B**) Representative clamp closing reactions for containing 40, 80, and 160 nM DNA (black traces) or DNA-SSB (blue traces) along with 20 nM γ complex clamp loader, 20 nM β-AF88$_2$, 200 nM unlabeled β, and 0.5 mM ATP. Solid red lines through the data show fits to a double exponential with values in Table 1. (**C**) Representative clamp closing reactions for 40 nM DNA-SSB substrates with 35, 65 or 80-nt ssDNA overhangs and 1.5 molar equivalents of SSB (darker shades of blue with increasing length). Clamp closing on the ss dT$_{80}$ substrate and 5 molar equivalents of SSB is shown in red.

fluorophores is separated and the relative fluorescence is high. When β-AF488$_2$ is closed on DNA, the AF488 fluorophores are within contact distance and fluorescence is quenched (62,65). The DNA substrate with a 30-bp duplex and a ss dT$_{65}$ 5′ overhang was used as in binding experiments. Rates of clamp closing by the γ complex clamp loader ($\gamma_3\delta\delta'\psi\chi$ subunits) were measured in sequential mixing stopped-flow experiments in which the clamp loader, clamp, and ATP were mixed and pre-incubated (4 s) to form a complex prior to addition of DNA or DNA-SSB and an excess of unlabeled clamps to limit reactions to a single measurable turnover (Figure 4A). Time courses for clamp closing are not exponential, but these data were fit to exponential decays to provide estimates of rates of decrease in fluorescence and to provide a measure of the reproducibility of experiments (Figure 4B). Addition of SSB to DNA did not affect the rates of clamp closing at the three different DNA concentrations (40, 80, and 160 nM) tested (Table 1). The rate of clamp loading is modestly dependent on the concentration of DNA or DNA-SSB. At the lowest concentration (40 nM) of DNA or DNA-SSB clamp closing is slower, but at the higher concentrations (80 and 160 nM) is the same within experimental error (Table 1). Given the modest concentration-dependence, clamp closing rates largely reflect the rate of an intramolecular reaction in the clamp loader-DNA complex.

The DNA substrate used in Figure 4B had a 65-nt ss DNA overhang so that SSB could potentially bind in any of the three most favored binding modes, (SSB)$_{35}$, (SSB)$_{56}$, or (SSB)$_{65}$. To determine whether differences in the SSB binding mode may affect the rate of clamp closing, the length of the ss DNA overhang and ratio of SSB to DNA was varied. Three different DNA substrates that differed in the length of the ss dT overhang, 35-, 65- or 80-nt were used. The

Table 1. Rates for clamp closing on DNA with a ss dT_{65} 5′ overhang

DNA-SSB (nM)	SSB	a_{fast}	k_{fast} (s^{-1})	a_{slow}	k_{slow} (s^{-1})
40	none	1 ± 0.1	7.5 ± 0.8	0.1 ± 0.04	1.1 ± 0.8
80	none	0.8 ± 0.2	10.7 ± 1.3	0.3 ± 0.2	3.1 ± 0.2
160	none	0.7 ± 0.2	13.1 ± 2.6	0.3 ± 0.2	3.9 ± 0.6
40	wt SSB	1 ± 0.1	7.6 ± 1.1	0.1 ± 0.05	1.5 ± 0.4
80	wt SSB	0.8 ± 0.1	10.9 ± 2.2	0.2 ± 0.06	3 ± 0.5
160	wt SSB	0.7 ± 0.1	16.3 ± 5.1	0.4 ± 0.1	4.5 ± 1.3
40	SSBΔC1	0.9 ± 0.1	1 ± 0.1	-	-
80	SSBΔC1	1 ± 0.04	2.3 ± 0.2	-	-
160	SSBΔC1	1 ± 0.05	3.5 ± 0.9	-	-

*Amplitudes (a) and rates (k) with standard deviations are given for three independent measurements.

Table 2. Rates for clamp closing reactions on DNA-SSB substrates (40 nM) with different lengths ss dT 5′ overhangs

5′ overhang	[SSB]/[DNA]	a_{fast}	k_{fast} (s^{-1})	a_{slow}	k_{slow} (s^{-1})
ss dT_{35}	1.5	1 ± 0.03	8.6 ± 0.4	0.1 ± 0.06	0.1 ± 0.05
ss dT_{65}	1.5	1 ± 0.05	9.1 ± 0.2	0.1 ± 0.09	0.4 ± 0.4
ss dT_{80}	1.5	1 ± 0.06	10.2 ± 0.1	0.05 ± 0.01	1.4 ± 0.4
ss dT_{80}	5	1 ± 0.04	8.7 ± 0.1	0.1 ± 0.05	0.4 ± 0.2

*Amplitudes (a) and rates (k) with standard deviations are given for three independent measurements.

ss dT_{35} substrate will only support binding in the $(SSB)_{35}$ binding mode and the ss dT_{80} substrate could potentially bind two molecules of SSB in the $(SSB)_{35}$ binding mode. All three DNA substrates had a 30-bp duplex of the same sequence. When 1.5 molecules of SSB per molecule of DNA (40 nM) was added to each, the rates of clamp closing were similar (Figure 4C and Table 2). When the number of SSB molecules was increased to 5 SSB molecules per ss dT_{80} DNA molecule to favor binding of 2 SSB molecules in the $(SSB)_{35}$ binding mode, the rate of clamp closing was similar to that for the reaction with 1.5 SSB molecules per DNA.

Clamp loading is inhibited by the SSB C-tail deletion mutant (SSBΔC1)

The binding affinity of the clamp loader for DNA bound by SSBΔC1 is lower than that for DNA bound by wt SSB. To determine how the SSBΔC1 mutant affects the activity of the clamp loader, clamp closing was measured on DNA-SSBΔC1. At the DNA concentrations tested (40, 80 and 160 nM), clamp closing on DNA bound by SSBΔC1 was slower than clamp closing on DNA bound by wt SSB and the rate of clamp closing increases with the concentration of DNA-SSBΔC1 (Figure 5 and Table 1). The increase in the rate scaled with the increase in DNA-SSBΔC1 concentration such that rates approximately double when the concentration doubled indicating that closing rates are dependent on binding rates.

The clamp loader efficiently remodels DNA-SSB to load clamps

Wild-type SSB on DNA does not impede clamp loader binding to DNA or loading clamps whereas the SSBΔC1 mutant inhibits both. This suggests that protein–protein interactions between the clamp loader and SSB allow the clamp loader to rapidly remodel DNA-SSB to gain access to the ss/ds DNA junction for efficient DNA binding and

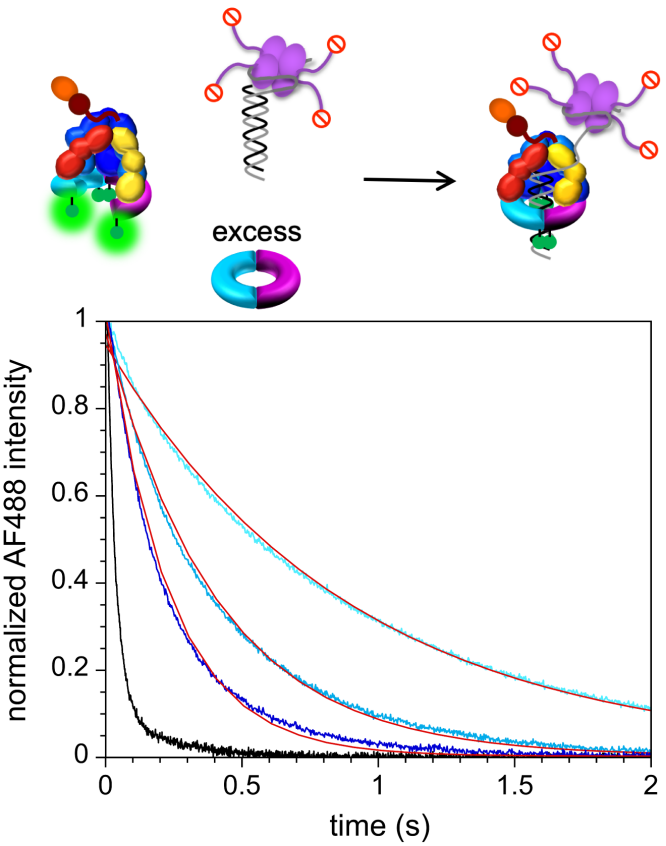

Figure 5. Clamp loading on DNA bound by SSBΔC1. Representative clamp closing time courses are shown for reactions containing 40, 80 or 160 nM DNA along with 1.5 equivalents of SSBΔC1 (darker blue with increasing concentration). Reactions also contain 20 nM γ complex clamp loader, 20 nM β-$AF488_2$, 200 nM unlabeled β, and 0.5 mM ATP. The black trace shows a clamp loading reaction on 'naked' DNA (160 nM) for comparison. Solid red lines show single exponential fits of the data with values reported in Table 1.

Table 3. Rates for clamp loader DNA binding and DNA-SSB remodeling on DNA with ss dT_{35}

Reaction	a_{fast}	k_{fast} (s^{-1})	a_{slow}	k_{slow} (s^{-1})
Binding	0.7 ± 0.06	10.9 ± 3.7	0.3 ± 0.06	0.9 ± 0.9
Remodeling	0.87 ± 0.10	10.4 ± 0.6	0.17 ± 0.04	0.8 ± 0.4

*Amplitudes (a) and rates (k) with standard deviations are given for three independent measurements.

clamp loading. This set of experiments measures DNA-SSB remodeling by the clamp loader directly by adapting a DNA-SSB remodeling assay previously used to measure SSB dynamics on DNA (63). Briefly, the primer strand annealed to ss dT_{35} DNA was labeled with a fluorescent donor, either AF488 or F, on the 30-nt duplex region 7-nt from the 3′ recessed end. SSB was labeled with an AF647 acceptor (SSB-AF647) at residue 122. When SSB-AF647 binds the DNA-AF488 donor, fluorescence is quenched. At saturating concentrations of SSB, there is about a 4- to 5-fold quench (4.5 ± 0.5) in donor fluorescence (Figure 6A). When the clamp loader, ATPγS, and the clamp are added, the donor fluorescence increases by about 1.5-fold (Figure 6B). This increase in donor fluorescence on clamp loader-clamp binding is small relative the magnitude of the quench that occurs when SSB-AF647 binds DNA-AF488 showing that the clamp loader does not completely displace SSB. Instead, DNA-SSB is remodeled in some way that moves the acceptor-labeled SSB farther from the donor on DNA when the clamp loader-clamp binds. DNA with a ss dT_{35} DNA overhang was used because clamp closing reactions were not strongly dependent on the length of the ss DNA overhang, and because the signal change for remodeling DNA-SSB is larger (1.5-fold) for ss dT_{35} DNA than for ss dT_{65} (1.2-fold).

DNA-SSB remodeling was measured in real time by adding a solution of γ complex and β to a solution of DNA-F bound by SSB-AF647, and the increase in donor fluorescence that occurs when the clamp loader remodels DNA-SSB was measured as a function of time. Time courses for DNA-SSB remodeling were overlayed on the time courses for DNA binding to define the temporal correlation between DNA binding and SSB-DNA remodeling (Figure 6C). This comparison along with rates calculated for the time courses show that DNA-SSB remodeling is rapid and occurs on the same time scale as clamp loader-DNA binding (Table 3).

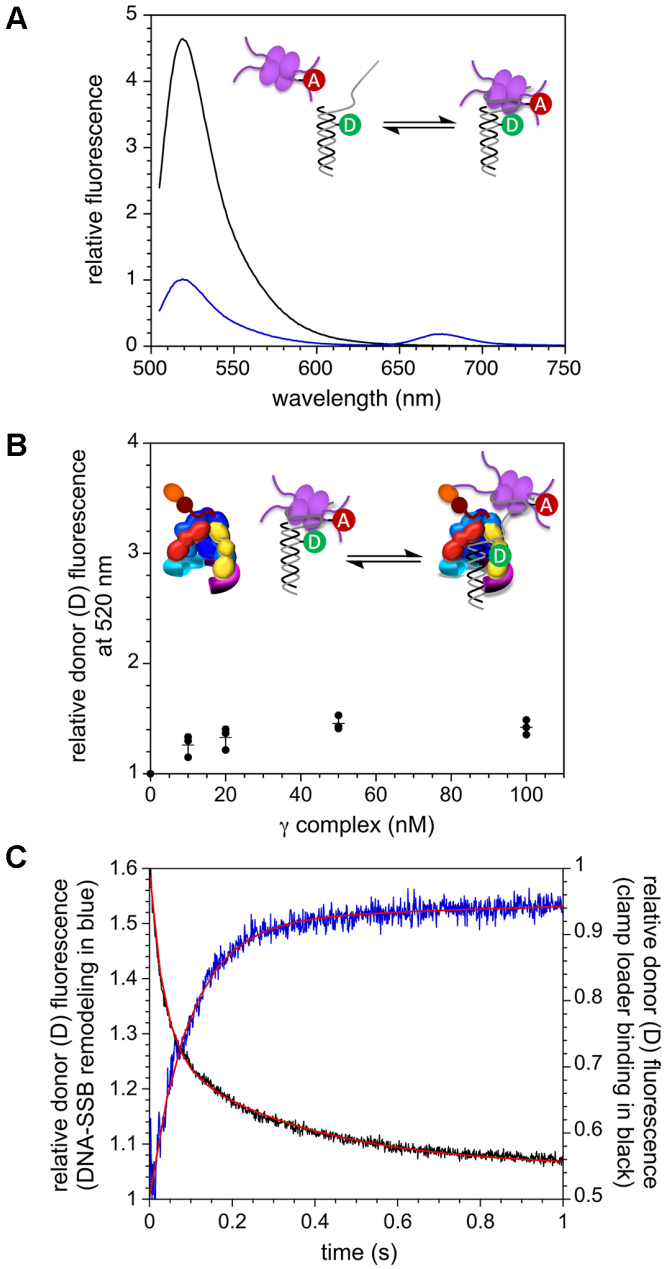

Figure 6. DNA-SSB remodeling by the clamp loader-clamp complex. (**A**) Representative fluorescence emission spectra are shown for 50 nM DNA-AF488 only (black) and 50 nM DNA-AF488 bound by SSB-AF647 (75 nM, blue). (**B**) The increase in donor (AF488) fluorescence that occurs when the clamp loader-clamp binds DNA-SSB-AF647 under equilibrium conditions is shown. Individual data points show donor fluorescence values for three independent experiments along with average values (horizontal lines) and standard deviations (error bars). (**C**) A representative time course for DNA-SSB remodeling when unlabeled γ complex (40 nM) and β (100 nM) are added to DNA-F (20 nM) bound by SSB-AF647 (30nM, blue) is overlayed on a time course for γ complex (40 nM) and β-AF647 (100 nM) binding DNA-F (20 nM, black).

DISCUSSION

Clamp loader binding DNA versus DNA-SSB

SSB can stimulate activities of enzymes that act on DNA, and we asked how SSB affected clamp loader–DNA binding and clamp loading activity. *In vivo*, SSB rapidly binds ssDNA that forms during DNA replication and would be bound on ssDNA adjacent to the ss/ds DNA junctions where clamps are loaded. Given that clamp loader's χ subunit physically interacts with the SSB C-tail, protein–protein interactions between the clamp loader and SSB (with 4 C-tails) bound adjacent to ss/ds DNA junctions could help to recruit the clamp loader to the right site on DNA. This was the case for RecQ helicase where SSB increases the on-rate for RecQ binding DNA (66). However, SSB had very little effect on the rates of clamp loader binding to DNA substrates with a 65-nt ssDNA overhang, and binding was modestly slower for DNA bound by SSB. It is

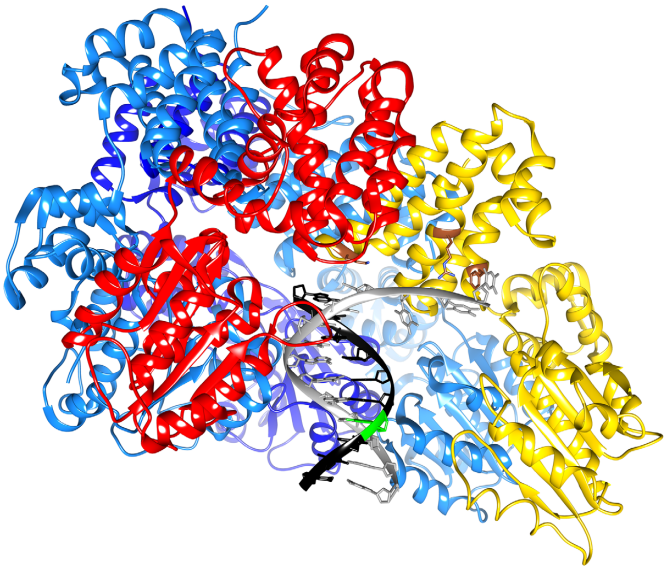

Figure 7. Ribbon diagram of a clamp loader ($\gamma_3\delta\delta$') bound to primer/template DNA (PDB ID: 3GLF (71)). The γ subunits are shown in shades of blue, δ' in red, and δ in gold. The DNA primer strand is black, the template strand is grey, and the nucleotide that is donor-labeled for FRET with AF647-labeled SSB is colored green. The five clamp loader subunits encircle the DNA duplex with the ss/ds DNA junction 'capped' by the clamp loader. Amino acid residues in the δ subunit (shown in brown) interact with the ssDNA overhang as it exits the clamp loader. The χ and ψ subunits present in the γ complex clamp loader used in this study are not present in this structure.

not surprising that SSB did not increase the binding rates because bimolecular rate constants for clamp loader-DNA binding to 'naked' DNA are already rapid and, the order of 1 to 6 × 10^8 M^{-1} s^{-1}, near the diffusion limit (56,67,68). Perhaps what is more surprising is that SSB does not substantially slow this rapid rate of DNA binding given that a stretch of DNA at the ss/ds DNA junction must be free for clamp loader binding. Structural data show that clamp loaders bind DNA in a manner that places the ss/ds DNA junction inside the 'cap' of the clamp loader with clamp loader subunits encircling about a helical turn of the duplex region (69–71) (Figure 7). When bound to DNA, the δ subunit of the *E. coli* clamp loader makes direct contact with the first four nucleotides of ssDNA at the ss/ds junction, and the volume of the clamp loader is likely to occlude a few more nucleotides of ssDNA (71). After the clamp loader-clamp is bound to DNA, SSB stabilizes the complex by increasing the lifetime of the clamp loader on DNA to increase the affinity of the clamp loader for DNA-SSB over naked DNA. This increased lifetime is consistent with the function of the χ-SSB interactions in the DNA polymerase III holoenzyme that generally stabilize the replicase at the replication fork (28,30,38).

Clamp loading on DNA versus DNA-SSB

SSB could also stimulate clamp loading activity by protein–protein interactions that have a positive allosteric effect on clamp loading activity. Previously, clamp loading on a symmetrical DNA substrate with two short 30-nt overhangs bound by SSB was measured, and SSB had little effect on rates of clamp closing (72). However, this DNA substrate was too short to allow SSB to bind in its preferred DNA binding modes, $(SSB)_{35}$, $(SSB)_{56}$ and $(SSB)_{65}$, in which DNA is wrapped around SSB to occlude 35-, 56- or 65-nucleotides, respectively. Therefore, we asked whether SSB stimulates clamp loading on a DNA substrate that is long enough to allow SSB to bind DNA in one of its preferred modes. The primary DNA substrate used in this study had a 65-nt ss dT overhang to allow SSB to bind DNA in any of these modes and to reduce DNA secondary structure that could potentially affect clamp loading on naked DNA. Clamp closing on DNA was used as a measure of clamp loading, and clamp closing rates were the same for DNA and DNA-SSB with a ss dT_{65} overhang. SSB neither stimulates nor inhibits clamp loading measured under single-turnover conditions in this clamp closing reaction.

The DNA binding mode of SSB depends on solution conditions including the salt concentration and the ratio of SSB to DNA. Low sodium chloride (10 mM NaCl) and high ratios of SSB to DNA favor the $(SSB)_{35}$ binding mode whereas high sodium chloride (≥200 mM NaCl) and magnesium chloride favor the $(SSB)_{65}$ binding mode (6–8). The assay buffer used here contained relatively high salt (50 mM NaCl and 8 mM $MgCl_2$) and a low SSB to DNA ratio (1.5:1 SSB:DNA) that likely favors the $(SSB)_{65}$ binding mode on the ss dT_{65} overhang. To determine whether clamp loading is influenced by the SSB DNA binding mode, clamp loading on DNA-SSB substrates with three different length overhangs, ss dT_{35}, ss dT_{65} and ss dT_{80}, was measured and with two different ratios of SSB to DNA on the longest ss dT_{80} substrate. At a SSB:DNA ratio of 1.5:1, the ss dT_{65} and ss dT_{80} substrates likely predominantly bind one SSB molecule in the $(SSB)_{65}$ binding mode. The ss dT_{35} substrate can only bind one SSB in the $(SSB)_{35}$ mode and a ratio of 5:1 SSB:DNA favors binding of two molecules of SSB to ss dT_{80} in the $(SSB)_{35}$ mode. Clamp closing rates were similar under these four conditions showing that the SSB binding mode does not have a large impact on clamp loading and the clamp loader can readily load clamps regardless of SSB or the binding mode. It should be noted that there was a modest increase in the clamp closing rate on increasing the length of ssDNA from 35- to 80-nt and a modest decrease in the closing rate when the number of molecules of SSB molecules per DNA was increased for the dT_{80} substrate. This could reflect a modest difference in the ability of the clamp loader to remodel SSB-DNA in the $(SSB)_{65}$ and $(SSB)_{35}$ binding modes. However, we believe that it more likely reflects the probability that there is a short stretch of ssDNA adjacent to the ss/ds DNA junction when the dT_{80} substrate is bound by a single SSB molecule.

In many of the studies showing that SSB stimulates enzymes, activity is measured in steady-state assays. Here, clamp loading was measured under pre-steady-state single-turnover conditions in clamp closing assays. In these reactions, the clamp loader binds DNA, hydrolyzes ATP, and closes the clamp around DNA. Clamp closing (and/or conformational changes required for clamp closing) is the slowest step in this single-turnover reaction, but clamp closing is not the rate-limiting step in the steady-state reaction cycle (56,73). Steady-state rates are likely limited by the rate of a dissociation event, clamp, DNA, or ADP dissociation

from the clamp loader, and it is possible that SSB affects the rate of one of these steps to affect clamp loading rates under steady-state conditions. There are also examples of SSB having an allosteric effect on enzymes to directly increase activity. The ATPase activity of RadD is directly stimulated by SSB (19), SSB stimulates the helicase activity of RecQ by promoting formation of a kinetic state that is capable of unwinding DNA faster than in the absence of SSB (74), and SSB exerts an allosteric effect on RecO that affects the oligomeric state of RecR-RecO to promote RecA loading onto DNA (75). Our single-turnover experiments would uncover a direct or allosteric effect on the clamp closing reaction if it were happening, but no such stimulation was measured.

Protein-Protein interactions and DNA-SSB remodeling

Even though SSB binds adjacent to ss/ds DNA junctions where clamps are loaded, SSB did not impede clamp loading even when the ssDNA overhang was relatively short (35 nt) leaving little room for another protein to bind. However, when protein–protein interactions between SSB and the χ subunit of the clamp loader are weakened by deletion of the C-terminal Phe of SSB, the SSBΔC1 mutant inhibits clamp loader-DNA interactions. Inhibition of enzyme activity by SSB C-tail mutants has been observed for other enzymes also (17,24,28,76). Binding of the clamp loader to DNA-SSBΔC1 was about 20-fold weaker than binding to DNA-SSB and clamp closing rates were also reduced (Figures 1 and 5). Not only is the rate of clamp closing slower on DNA-SSBΔC1 than DNA-SSB, but the rate was linearly dependent on the concentration of DNA-SSBΔC1 (Table 1). This shows that slowest step in the pre-steady-state clamp closing reaction changed from an intramolecular clamp closing step for reactions with wt SSB to a biomolecular DNA binding reaction for DNA-SSBΔC1. In other words, SSBΔC1 inhibits DNA binding so that the binding reaction becomes rate-limiting in single-turnover clamp closing reactions. SSB-DNA interactions are dynamic in that even though SSB binds DNA tightly, SSB moves along DNA and can switch between binding modes which ultimately changes the 'footprint' of SSB to uncover ssDNA (10,11) and deletion of the C-terminal Phe is unlikely to affect SSB-DNA dynamics because this Phe is not in the DNA binding domain. These dynamics likely permit the clamp loader to load clamps on DNA-SSBΔC1 albeit at a slower rate. Rapid clamp loading requires protein–protein interactions between the clamp loader and SSB that allow the clamp loader to actively remodel DNA-SSB.

Perhaps the most striking result of this work is that DNA-SSB remodeling by the clamp loader is so rapid and efficient such that DNA binding rates and clamp closing are not substantially different for DNA and DNA-SSB. This was verified by measuring DNA-SSB remodeling directly using a FRET-based assay under identical conditions to reactions measuring the clamp loader binding to DNA-SSB. These experiments showed DNA-SSB remodeling occurs on a similar time scale as the DNA binding reaction (Figure 6 and Table 3). The other interesting result from DNA-SSB remodeling reactions was that both the clamp loader and SSB can bind to DNA even when the ssDNA overhang is as short as 35 nt. When acceptor-labeled SSB binds donor-labeled DNA, there was about a 4 to 5-fold quench in fluorescence. If SSB had been displaced from DNA completely, donor fluorescence should have increased by 4 to 5 times but fluorescence only increased about 1.5-fold. While these experiments show that SSB is still bound to DNA, the magnitude of the decrease in FRET may not represent the average distance that SSB has moved along ssDNA away from the donor because the clamp loader bends ssDNA (Figure 7). Bending of ssDNA that occurs when the clamp loader binds likely places SSB in closer proximity to the donor in 3D space to increase FRET and partially offset the decrease in FRET due the increase in the number of nucleotides between SSB and the donor on DNA.

The major mode of SSB binding to partner proteins (SIPs) is via protein–protein interactions between the conserved C-tail of SSB and the SIP (reviewed in (1,5)). The C-terminal end of SSB starting at about residue 112 (of 177 total amino acid residues) is intrinsically disordered and is often depicted as an unfolded flexible rope-like structure as in our diagrams (77–79). If this were the case, it seems unlikely that the clamp loader and other SSB binding proteins would be able to bind the C-tail and effectively remodel DNA-SSB. A more rigid structure within the disordered region of SSB would allow proteins to push on SSB to remodel DNA-SSB to create space on ssDNA to bind. Molecular modeling studies suggest that although the disordered region does not fold into a regular structure, it does collapse into a globular state (80). This may provide the rigidity needed for DNA-SSB remodeling. Another interesting possibility is that interaction of the C-tail with a SSB binding partner induces the intrinsically disordered region to become structured.

Single-molecule studies suggest that SSB binding partners can remodel DNA-SSB by shifting the binding mode from $(SSB)_{65}$ to $(SSB)_{35}$ exposing a region of ssDNA (23,26,63,66). While our ensemble FRET measurements cannot distinguish between binding modes, they do address the timing of DNA-SSB remodeling which is not addressed in single molecule experiments. The timing of DNA-SSB remodeling binding shows that the clamp loader actively remodels DNA-SSB on binding rather than binding DNA-SSB that has spontaneously rearranged which is supported by experiments with the SSB deletion mutant, SSBΔC1. If the clamp loader were taking advantage of spontaneous DNA-SSB rearrangements, then the SSBΔC1 mutant would not have been inhibitory. Thus, protein–protein interactions between the clamp loader and SSB facilitate rapid and efficient remodeling so that clamp loading occurs at rates that are not impeded by the presence of SSB bound to DNA.

DATA AVAILABILITY

The data underlying this article are available in this article. Expression plasmids for proteins used in this study and raw data will be shared upon request to the corresponding author.

ACKNOWLEDGEMENTS

We thank the Keck laboratory for providing an expression vector for SSBΔC1.

FUNDING

National Science Foundation [MCB 1817869 to L.B.B.]. Funding for open access charge: National Science Foundation.
Conflict of interest statement. None declared.

REFERENCES

1. Antony,E. and Lohman,T.M. (2019) Dynamics of *E. coli* single stranded DNA binding (SSB) protein-DNA complexes. *Semin. Cell. Dev. Biol.*, **86**, 102–111.
2. Chen,R. and Wold,M.S. (2014) Replication protein A: single-stranded DNA's first responder: dynamic DNA-interactions allow replication protein A to direct single-strand DNA intermediates into different pathways for synthesis or repair. *Bioessays*, **36**, 1156–1161.
3. Marceau,A.H. (2012) Functions of single-strand DNA-binding proteins in DNA replication, recombination, and repair. *Methods Mol. Biol.*, **922**, 1–21.
4. Fanning,E., Klimovich,V. and Nager,A.R. (2006) A dynamic model for replication protein A (RPA) function in DNA processing pathways. *Nucleic Acids Res.*, **34**, 4126–4137.
5. Shereda,R.D., Kozlov,A.G., Lohman,T.M., Cox,M.M. and Keck,J.L. (2008) SSB as an organizer/mobilizer of genome maintenance complexes. *Crit. Rev. Biochem. Mol. Biol.*, **43**, 289–318.
6. Bujalowski,W. and Lohman,T.M. (1986) *Escherichia coli* single-strand binding protein forms multiple, distinct complexes with single-stranded DNA. *Biochemistry*, **25**, 7799–7802.
7. Bujalowski,W., Overman,L.B. and Lohman,T.M. (1988) Binding mode transitions of *Escherichia coli* single strand binding protein-single-stranded DNA complexes. Cation, anion, pH, and binding density effects. *J. Biol. Chem.*, **263**, 4629–4640.
8. Lohman,T.M. and Overman,L.B. (1985) Two binding modes in *Escherichia coli* single strand binding protein-single stranded DNA complexes. Modulation by NaCl concentration. *J. Biol. Chem.*, **260**, 3594–3603.
9. Overman,L.B., Bujalowski,W. and Lohman,T.M. (1988) Equilibrium binding of *Escherichia coli* single-strand binding protein to single-stranded nucleic acids in the (SSB)65 binding mode. Cation and anion effects and polynucleotide specificity. *Biochemistry*, **27**, 456–471.
10. Roy,R., Kozlov,A.G., Lohman,T.M. and Ha,T. (2007) Dynamic structural rearrangements between DNA binding modes of *E. coli* SSB protein. *J. Mol. Biol.*, **369**, 1244–1257.
11. Zhou,R., Kozlov,A.G., Roy,R., Zhang,J., Korolev,S., Lohman,T.M. and Ha,T. (2011) SSB functions as a sliding platform that migrates on DNA via reptation. *Cell*, **146**, 222–232.
12. Arad,G., Hendel,A., Urbanke,C., Curth,U. and Livneh,Z. (2008) Single-stranded DNA-binding protein recruits DNA polymerase V to primer termini on RecA-coated DNA. *J. Biol. Chem.*, **283**, 8274–8282.
13. Furukohri,A., Nishikawa,Y., Akiyama,M.T. and Maki,H. (2012) Interaction between *Escherichia coli* DNA polymerase IV and single-stranded DNA-binding protein is required for DNA synthesis on SSB-coated DNA. *Nucleic Acids Res.*, **40**, 6039–6048.
14. Naue,N., Beerbaum,M., Bogutzki,A., Schmieder,P. and Curth,U. (2013) The helicase-binding domain of *Escherichia coli* DnaG primase interacts with the highly conserved C-terminal region of single-stranded DNA-binding protein. *Nucleic Acids Res.*, **41**, 4507–4517.
15. Lu,D. and Keck,J.L. (2008) Structural basis of *Escherichia coli* single-stranded DNA-binding protein stimulation of exonuclease I. *Proc. Natl. Acad. Sci. U.S.A.*, **105**, 9169–9174.
16. Petzold,C., Marceau,A.H., Miller,K.H., Marqusee,S. and Keck,J.L. (2015) Interaction with single-stranded DNA-binding protein stimulates *Escherichia coli* ribonuclease HI enzymatic activity. *J. Biol. Chem.*, **290**, 14626–14636.
17. Cheng,Z., Caillet,A., Ren,B. and Ding,H. (2012) Stimulation of *Escherichia coli* DNA damage inducible DNA helicase DinG by the single-stranded DNA binding protein SSB. *FEBS Lett.*, **586**, 3825–3830.
18. Shereda,R.D., Reiter,N.J., Butcher,S.E. and Keck,J.L. (2009) Identification of the SSB binding site on *E. coli* RecQ reveals a conserved surface for binding SSB's C terminus. *J. Mol. Biol.*, **386**, 612–625.
19. Chen,S.H., Byrne-Nash,R.T. and Cox,M.M. (2016) *Escherichia coli* RadD protein functionally interacts with the single-stranded DNA-binding protein. *J. Biol. Chem.*, **291**, 20779–20786.
20. Hobbs,M.D., Sakai,A. and Cox,M.M. (2007) SSB protein limits RecOR binding onto single-stranded DNA. *J. Biol. Chem.*, **282**, 11058–11067.
21. Page,A.N., George,N.P., Marceau,A.H., Cox,M.M. and Keck,J.L. (2011) Structure and biochemical activities of *Escherichia coli* MgsA. *J. Biol. Chem.*, **286**, 12075–12085.
22. Umezu,K. and Kolodner,R.D. (1994) Protein interactions in genetic recombination in *Escherichia coli*. Interactions involving RecO and RecR overcome the inhibition of RecA by single-stranded DNA-binding protein. *J. Biol. Chem.*, **269**, 30005–30013.
23. Bhattacharyya,B., George,N.P., Thurmes,T.M., Zhou,R., Jani,N., Wessel,S.R., Sandler,S.J., Ha,T. and Keck,J.L. (2014) Structural mechanisms of PriA-mediated DNA replication restart. *Proc. Natl. Acad. Sci. U.S.A.*, **111**, 1373–1378.
24. Cadman,C.J. and McGlynn,P. (2004) PriA helicase and SSB interact physically and functionally. *Nucleic Acids Res.*, **32**, 6378–6387.
25. Kozlov,A.G., Jezewska,M.J., Bujalowski,W. and Lohman,T.M. (2010) Binding specificity of *Escherichia coli* single-stranded DNA binding protein for the chi subunit of DNA pol III holoenzyme and PriA helicase. *Biochemistry*, **49**, 3555–3566.
26. Wessel,S.R., Marceau,A.H., Massoni,S.C., Zhou,R., Ha,T., Sandler,S.J. and Keck,J.L. (2013) PriC-mediated DNA replication restart requires PriC complex formation with the single-stranded DNA-binding protein. *J. Biol. Chem.*, **288**, 17569–17578.
27. Handa,P., Acharya,N. and Varshney,U. (2001) Chimeras between single-stranded DNA-binding proteins from *Escherichia coli* and *mycobacterium tuberculosis* reveal that their C-terminal domains interact with uracil DNA glycosylases. *J. Biol. Chem.*, **276**, 16992–16997.
28. Kelman,Z., Yuzhakov,A., Andjelkovic,J. and O'Donnell,M. (1998) Devoted to the lagging strand-the chi subunit of DNA polymerase III holoenzyme contacts SSB to promote processive elongation and sliding clamp assembly. *EMBO J.*, **17**, 2436–2449.
29. Witte,G., Urbanke,C. and Curth,U. (2003) DNA polymerase III chi subunit ties single-stranded DNA binding protein to the bacterial replication machinery. *Nucleic Acids Res.*, **31**, 4434–4440.
30. Marceau,A.H., Bahng,S., Massoni,S.C., George,N.P., Sandler,S.J., Marians,K.J. and Keck,J.L. (2011) Structure of the SSB-DNA polymerase III interface and its role in DNA replication. *EMBO J.*, **30**, 4236–4247.
31. Naue,N., Fedorov,R., Pich,A., Manstein,D.J. and Curth,U. (2011) Site-directed mutagenesis of the chi subunit of DNA polymerase III and single-stranded DNA-binding protein of *E. coli* reveals key residues for their interaction. *Nucleic Acids Res.*, **39**, 1398–1407.
32. Ryzhikov,M., Koroleva,O., Postnov,D., Tran,A. and Korolev,S. (2011) Mechanism of RecO recruitment to DNA by single-stranded DNA binding protein. *Nucleic Acids Res.*, **39**, 6305–6314.
33. Curth,U., Genschel,J., Urbanke,C. and Greipel,J. (1996) *In vitro* and *in vivo* function of the C-terminus of *Escherichia coli* single-stranded DNA binding protein. *Nucleic Acids Res.*, **24**, 2706–2711.
34. Bianco,P.R. and Lyubchenko,Y.L. (2017) SSB and the RecG DNA helicase: an intimate association to rescue a stalled replication fork. *Protein Sci.*, **26**, 638–649.
35. Bianco,P.R., Pottinger,S., Tan,H.Y., Nguyenduc,T., Rex,K. and Varshney,U. (2017) The IDL of *E. coli* SSB links ssDNA and protein binding by mediating protein–protein interactions. *Protein Sci.*, **26**, 227–241.
36. Ding,W., Tan,H.Y., Zhang,J.X., Wilczek,L.A., Hsieh,K.R., Mulkin,J.A. and Bianco,P.R. (2020) The mechanism of single strand binding protein-RecG binding: Implications for SSB interactome function. *Protein Sci.*, **29**, 1211–1227.
37. Nigam,R., Mohan,M., Shivange,G., Dewangan,P.K. and Anindya,R. (2018) *Escherichia coli* AlkB interacts with single-stranded DNA binding protein SSB by an intrinsically disordered region of SSB. *Mol. Biol. Rep.*, **45**, 865–870.
38. Glover,B.P. and McHenry,C.S. (1998) The chi psi subunits of DNA polymerase III holoenzyme bind to single-stranded DNA-binding protein (SSB) and facilitate replication of an SSB-coated template. *J. Biol. Chem.*, **273**, 23476–23484.

39. Downey,C.D. and McHenry,C.S. (2010) Chaperoning of a replicative polymerase onto a newly assembled DNA-bound sliding clamp by the clamp loader. *Mol. Cell.*, **37**, 481–491.
40. Yuzhakov,A., Kelman,Z. and O'Donnell,M. (1999) Trading places on DNA – a three-point switch underlies primer handoff from primase to the replicative DNA polymerase. *Cell*, **96**, 153–163.
41. Pritchard,A.E., Dallmann,H.G., Glover,B.P. and McHenry,C.S. (2000) A novel assembly mechanism for the DNA polymerase III holoenzyme DnaX complex: association of deltadelta' with DnaX(4) forms DnaX(3)deltadelta'. *EMBO J.*, **19**, 6536–6545.
42. Park,A.Y., Jergic,S., Politis,A., Ruotolo,B.T., Hirshberg,D., Jessop,L.L., Beck,J.L., Barsky,D., O'Donnell,M., Dixon,N.E. *et al.* (2010) A single subunit directs the assembly of the *Escherichia coli* DNA sliding clamp loader. *Structure*, **18**, 285–292.
43. Blinkowa,A.L. and Walker,J.R. (1990) Programmed ribosomal frameshifting generates the Escherichia coli DNA polymerase III gamma subunit from within the tau subunit reading frame. *Nucleic Acids Res.*, **18**, 1725–1729.
44. Flower,A.M. and McHenry,C.S. (1990) The gamma subunit of DNA polymerase III holoenzyme of *Escherichia coli* is produced by ribosomal frameshifting. *Proc. Natl. Acad. Sci. U.S.A.*, **87**, 3713–3717.
45. Tsuchihashi,Z. and Kornberg,A. (1990) Translational frameshifting generates the gamma subunit of DNA polymerase III holoenzyme. *Proc. Natl. Acad. Sci. U.S.A.*, **87**, 2516–2520.
46. Gao,D. and McHenry,C.S. (2001) tau binds and organizes *Escherichia coli* replication proteins through distinct domains. Domain IV, located within the unique C terminus of tau, binds the replication fork, helicase, DnaB. *J. Biol. Chem.*, **276**, 4441–4446.
47. Gao,D. and McHenry,C.S. (2001) tau binds and organizes *Escherichia coli* replication through distinct domains. Partial proteolysis of terminally tagged tau to determine candidate domains and to assign domain V as the alpha binding domain. *J. Biol. Chem.*, **276**, 4433–4440.
48. Kim,S., Dallmann,H.G., McHenry,C.S. and Marians,K.J. (1996) Coupling of a replicative polymerase and helicase: a tau-DnaB interaction mediates rapid replication fork movement. *Cell*, **84**, 643–650.
49. McHenry,C.S. (1982) Purification and characterization of DNA polymerase III'. Identification of tau as a subunit of the DNA polymerase III holoenzyme. *J. Biol. Chem.*, **257**, 2657–2663.
50. Studwell-Vaughan,P.S. and O'Donnell,M. (1991) Constitution of the twin polymerase of DNA polymerase III holoenzyme. *J. Biol. Chem.*, **266**, 19833–19841.
51. Yuzhakov,A., Turner,J. and O'Donnell,M. (1996) Replisome assembly reveals the basis for asymmetric function in leading and lagging strand replication. *Cell*, **86**, 877–886.
52. Jergic,S., Ozawa,K., Williams,N.K., Su,X.C., Scott,D.D., Hamdan,S.M., Crowther,J.A., Otting,G. and Dixon,N.E. (2007) The unstructured C-terminus of the tau subunit of *Escherichia coli* DNA polymerase III holoenzyme is the site of interaction with the alpha subunit. *Nucleic Acids Res.*, **35**, 2813–2824.
53. Su,X.C., Jergic,S., Keniry,M.A., Dixon,N.E. and Otting,G. (2007) Solution structure of domains iva and V of the tau subunit of *Escherichia coli* DNA polymerase III and interaction with the alpha subunit. *Nucleic Acids Res.*, **35**, 2825–2832.
54. Dohrmann,P.R., Correa,R., Frisch,R.L., Rosenberg,S.M. and McHenry,C.S. (2016) The DNA polymerase III holoenzyme contains gamma and is not a trimeric polymerase. *Nucleic Acids Res.*, **44**, 1285–1297.
55. McInerney,P., Johnson,A., Katz,F. and O'Donnell,M. (2007) Characterization of a triple DNA polymerase replisome. *Mol. Cell.*, **27**, 527–538.
56. Anderson,S.G., Thompson,J.A., Paschall,C.O., O'Donnell,M. and Bloom,L.B. (2009) Temporal correlation of DNA binding, ATP hydrolysis, and clamp release in the clamp loading reaction catalyzed by the *Escherichia coli* gamma complex. *Biochemistry*, **48**, 8516–8527.
57. Douma,L.G., Yu,K.K., England,J.K., Levitus,M. and Bloom,L.B. (2017) Mechanism of opening a sliding clamp. *Nucleic Acids Res.*, **45**, 10178–10189.
58. Johanson,K.O., Haynes,T.E. and McHenry,C.S. (1986) Chemical characterization and purification of the beta subunit of the DNA polymerase III holoenzyme from an overproducing strain. *J. Biol. Chem.*, **261**, 11460–11465.
59. Yao,N., Hurwitz,J. and O'Donnell,M. (2000) Dynamics of beta and proliferating cell nuclear antigen sliding clamps in traversing DNA secondary structure. *J. Biol. Chem.*, **275**, 1421–1432.
60. Williams,C.R., Snyder,A.K., Kuzmic,P., O'Donnell,M. and Bloom,L.B. (2004) Mechanism of loading the *Escherichia coli* DNA polymerase III sliding clamp: I. Two distinct activities for individual ATP sites in the gamma complex. *J. Biol. Chem.*, **279**, 4376–4385.
61. Bloom,L.B., Turner,J., Kelman,Z., Beechem,J.M., O'Donnell,M. and Goodman,M.F. (1996) Dynamics of loading the beta sliding clamp of DNA polymerase III onto DNA. *J. Biol. Chem.*, **271**, 30699–30708.
62. Paschall,C.O., Thompson,J.A., Marzahn,M.R., Chiraniya,A., Hayner,J.N., O'Donnell,M., Robbins,A.H., McKenna,R. and Bloom,L.B. (2011) The *Escherichia coli* clamp loader can actively pry open the beta-sliding clamp. *J. Biol. Chem.*, **286**, 42704–42714.
63. Roy,R., Kozlov,A.G., Lohman,T.M. and Ha,T. (2009) SSB protein diffusion on single-stranded DNA stimulates RecA filament formation. *Nature*, **461**, 1092–1097.
64. Naktinis,V., Onrust,R., Fang,L. and O'Donnell,M. (1995) Assembly of a chromosomal replication machine: two DNA polymerases, a clamp loader, and sliding clamps in one holoenzyme particle. II. Intermediate complex between the clamp loader and its clamp. *J. Biol. Chem.*, **270**, 13358–13365.
65. Donaphon,B., Bloom,L.B. and Levitus,M. (2018) Photophysical characterization of interchromophoric interactions between rhodamine dyes conjugated to proteins. *Methods Appl. Fluoresc.*, **6**, 045004.
66. Mills,M., Harami,G.M., Seol,Y., Gyimesi,M., Martina,M., Kovacs,Z.J., Kovacs,M. and Neuman,K.C. (2017) RecQ helicase triggers a binding mode change in the SSB-DNA complex to efficiently initiate DNA unwinding. *Nucleic Acids Res.*, **45**, 11878–11890.
67. Ason,B., Bertram,J.G., Hingorani,M.M., Beechem,J.M., O'Donnell,M., Goodman,M.F. and Bloom,L.B. (2000) A model for Escherichia coli DNA polymerase III holoenzyme assembly at primer/template ends. DNA triggers a change in binding specificity of the gamma complex clamp loader. *J. Biol. Chem.*, **275**, 3006–3015.
68. Bertram,J.G., Bloom,L.B., Hingorani,M.M., Beechem,J.M., O'Donnell,M. and Goodman,M.F. (2000) Molecular mechanism and energetics of clamp assembly in Escherichia coli. The role of ATP hydrolysis when gamma complex loads beta on DNA. *J. Biol. Chem.*, **275**, 28413–28420.
69. Kelch,B.A., Makino,D.L., O'Donnell,M. and Kuriyan,J. (2011) How a DNA polymerase clamp loader opens a sliding clamp. *Science*, **334**, 1675–1680.
70. Miyata,T., Suzuki,H., Oyama,T., Mayanagi,K., Ishino,Y. and Morikawa,K. (2005) Open clamp structure in the clamp-loading complex visualized by electron microscopic image analysis. *Proc. Natl. Acad. Sci. U.S.A.*, **102**, 13795–13800.
71. Simonetta,K.R., Kazmirski,S.L., Goedken,E.R., Cantor,A.J., Kelch,B.A., McNally,R., Seyedin,S.N., Makino,D.L., O'Donnell,M. and Kuriyan,J. (2009) The mechanism of ATP-dependent primer-template recognition by a clamp loader complex. *Cell*, **137**, 659–671.
72. Hayner,J.N., Douma,L.G. and Bloom,L.B. (2014) The interplay of primer-template DNA phosphorylation status and single-stranded DNA binding proteins in directing clamp loaders to the appropriate polarity of DNA. *Nucleic Acids Res.*, **42**, 10655–10667.
73. Hayner,J.N. and Bloom,L.B. (2013) The beta sliding clamp closes around DNA prior to release by the *Escherichia coli* clamp loader gamma complex. *J. Biol. Chem.*, **288**, 1162–1170.
74. Bagchi,D., Manosas,M., Zhang,W., Manthei,K.A., Hodeib,S., Ducos,B., Keck,J.L. and Croquette,V. (2018) Single molecule kinetics uncover roles for *E. coli* RecQ DNA helicase domains and interaction with SSB. *Nucleic Acids Res.*, **46**, 8500–8515.
75. Shinn,M.K., Kozlov,A.G. and Lohman,T.M. (2021) Allosteric effects of SSB C-terminal tail on assembly of *E. coli* RecOR proteins. *Nucleic Acids Res.*, **49**, 1987–2004.
76. Shereda,R.D., Bernstein,D.A. and Keck,J.L. (2007) A central role for SSB in *Escherichia coli* RecQ DNA helicase function. *J. Biol. Chem.*, **282**, 19247–19258.
77. Raghunathan,S., Kozlov,A.G., Lohman,T.M. and Waksman,G. (2000) Structure of the DNA binding domain of *E. coli* SSB bound to ssDNA. *Nat. Struct. Biol.*, **7**, 648–652.

78. Savvides,S.N., Raghunathan,S., Futterer,K., Kozlov,A.G., Lohman,T.M. and Waksman,G. (2004) The C-terminal domain of full-length *E. coli* SSB is disordered even when bound to DNA. *Protein Sci.*, **13**, 1942–1947.
79. Williams,K.R., Spicer,E.K., LoPresti,M.B., Guggenheimer,R.A. and Chase,J.W. (1983) Limited proteolysis studies on the *Escherichia coli* single-stranded DNA binding protein. Evidence for a functionally homologous domain in both the *Escherichia coli* and T4 DNA binding proteins. *J. Biol. Chem.*, **258**, 3346–3355.
80. Kozlov,A.G., Weiland,E., Mittal,A., Waldman,V., Antony,E., Fazio,N., Pappu,R.V. and Lohman,T.M. (2015) Intrinsically disordered C-terminal tails of *E. coli* single-stranded DNA binding protein regulate cooperative binding to single-stranded DNA. *J. Mol. Biol.*, **427**, 763–774.